Title
Corrosion Resistant Coatings for High-Temperature High-Sulfur-Activity Applications

Author
Selman, J.R.

Publication Date
1994-02-01

LBL-35339
UC-331

Lawrence Berkeley Laboratory
UNIVERSITY OF CALIFORNIA

ENERGY & ENVIRONMENT DIVISION

Corrosion-Resistant Coatings for High-Temperature High-Sulfur-Activity Applications

J.R. Selman

February 1994

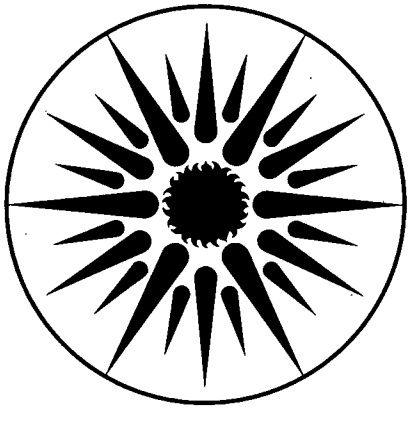

ENERGY & ENVIRONMENT DIVISION

Prepared for the U.S. Department of Energy under Contract Number DE-AC03-76SF00098

DISCLAIMER

LBL-35339

CORROSION-RESISTANT COATINGS FOR HIGH-TEMPERATURE HIGH-SULFUR-ACTIVITY APPLICATIONS

Final Report

February 1994

by

J.R. Selman

Illinois Institute of Technology
Department of Chemical Engineering
Chicago, Illinois 60616

for

Exploratory Technology Research Program
Energy & Environment Division
Lawrence Berkeley Laboratory
Berkeley, California 94720

This work was supported by the Assistant Secretary for Energy Efficiency and Renewable Energy, Office of Transportation Technologies, Electric and Hybrid Propulsion Division of the U.S. Department of Energy under Contract No. DE-AC03-76SF00098, Subcontract No. 4578210 with the Lawrence Berkeley Laboratory.

SUMMARY

Introduction

The research described in this report is intended to assistant in developing the technology for the production of molybdenum and molybdenum carbide coatings. These coatings have the potential to serve as an alternative to present methods of protecting metal parts at positive potential, of high-temperature sulfur or sulfide batteries.

Two methods have been employed as follows;

Task 1. Study of Molybdenum Carbide Electrodeposition from Oxide Based Molten Salts

Dense, well-adherent molybdenum carbide coatings have been deposited on mild steel substrates by electrochemical deposition from a Na_2WO_4 - K_2WO_4 molten bath containing alkali molybdates and carbonates. Coatings with thicknesses up to 30 μm have been prepared at cathodic current densities between 30 and 50 $mA.cm^{-2}$ under air as ambient atmosphere. The coating morphology depends strongly on melt composition, temperature and moisture content. Addition of $Na_2B_4O_7$ to the basic non-lithium bath composition causes significant quality and morphology improvements. It is shown that the initial stages of the molybdenum carbide electrodeposition can be described by a model involving instantaneous nucleation and 3-D diffusion-controlled growth.

Task 2. Preparation of Mo and Mo_2C by Plasma-Enhanced Chemical Vapor Deposition

New applications of molybdenum carbide films can exploit the unique properties of plasma enhanced CVD films deposited at relatively low temperature. Using factorial experimental design, a series of experiments has been carried out to investigate the PECVD process with $Mo(CO)_6$ as a precursor. Information about the effects of the chamber pressure, saturator temperature, gas composition and gas flow rate was obtained by experiments. Elemental analysis of the thin film was carried out by Auger electron spectroscopy. Further investigations are being carried out on the basis of thermodynamics, heterogeneous kinetics, and mass transport, in conjunction with measurements of evaporation rate and analysis of the solid and gaseous phases.

Introduction

The research described in this report is intended to assist in developing technology for the production of molybdenum and molybdenum carbide coatings. These coatings have the potential to serve as an alternative to present methods of protecting metal parts at positive potential, of high-temperature sulfur or sulfide batteries.

Two methods have been employed as follows;

Task 1. Molybdenum Carbide Electrodeposition from Oxide Based Molten Salts

Recently, considerable attention has been focused on the development of coatings of molybdenum and molybdenum carbide by molten salt electrochemical deposition (MSECD). These coatings are considered candidate materials for coating the container and positive-electrode current collector of high-temperature power sources such as sodium/sulfur and lithium/FeS_2 batteries.

MSECD is a powerful method which can be used to produce various compound-based coatings having improved properties compared with those of pure elements. This method offers the ability to coat complex shapes and provides good process control by precise current/potential variation.

Formation of refractory metal and metal carbide deposits by MSECD using several different bath composition (chloride, chloride-oxide, fluoride) has been demonstrated by many authors (1-11). However, all of these methods have difficulties in practical use, connected mainly with the inert atmosphere needed, complicated treating steps, special purity requirements for the electrolyte baths, etc. Recently, a new method was proposed, using non-fluoride based electrochemical deposition from a melt consisting completely of oxides, with air as ambient atmosphere (12-16). The method can be summarized as follows. Mo_2C coatings are deposited directly on mild steel from a Na_2WO_4-K_2WO_4-Li_2MoO_4-Li_2CO_3 melt at 900°C. Dense coatings with thicknesses up to 50 μm are obtained at cathodic current densities between 20 and 100 $mA.cm^{-2}$. The authors attribute the deposition of Mo_2C from oxide melts to the simultaneous chemical reaction of carbon and molybdenum produced from the corresponding oxygenated anions. As a result of this reaction a compact pore-free deposit of molybdenum carbide is obtained with good adhesion to the low-carbon steel substrate. Preliminary results on the

corrosion and electrochemical behavior of Mo_2C coatings deposited electrochemically on low carbon steel showed good promise for corrosion protection of the cathode container of sodium/sulfur batteries (17).

Task 2. Preparation of Mo and Mo_2C by Plasma-Enhanced Chemical Vapor Deposition

Plasma-enhanced chemical vapor deposition (PECVD) has found application as a new technique for preparing thin protective films at much lower temperatures than by thermally driven CVD. This low-temperature capability is due to the addition of plasma energy to the CVD environment in the form of a glow discharge, which creates highly reactive species. New applications of molybdenum or molybdenum carbide films can exploit the unique properties of PECVD films deposited at relatively low temperature. An effort has been undertaken to deposit Mo and Mo_2C films on a substrate of glass or steel.

A series of experiments has been carried out to investigate the evaporation mechanism of molybdenum carbonyl as a precursor. The following experimental parameters were varied: pressure (P), temperature (T), RF power, time (t), gas composition and gas flow rate. The PECVD film was characterized by a variety of analytical techniques. X-ray diffraction spectrometry was used to determine the structure of the films. Scanning electron micrographs were taken to determine the film thickness and morphology. X-ray photoelectron spectroscopy and energy dispersive spectrometry helped to determine the chemical composition of films.

Fundamental investigation must be carried out on the basis of theoretical approaches such as thermodynamics, heterogeneous kinetics, and mass transport. A thermodynamic program was used to predict process efficiency under various process conditions and the predictions were compared with the experimental data.

Research Objectives

Task 1. The objectives of this study are to produce dense and adherent molybdenum carbide coatings from sodium tungstate-potassium tungstate based melts, and to determine correlations with process parameters such as temperature, current density, melt composition, moisture content etc. Since it is well known that the initial stages of electrodeposition on foreign substrates determine to a great extent the morphology and the properties of the corresponding

coatings, additional preliminary investigations were performed in order to clarify the mechanism and kinetics of nucleation and growth of the molybdenum carbide.

Task 2. This task is aimed at advancing the preparation and characterization of thin films of molybdenum and molybdenum carbide by low temperature, plasma enhanced chemical vapor deposition (PECVD). The emphasis is on the properties of thin films of molybdenum and molybdenum carbides; the effect of experimental variables on film properties; and, the correlation between experimental variables. In summary, the objectives of this research are as follows:

(1) Elucidation of the mechanism of molybdenum and molybdenum carbide deposition by PECVD;

(2) An investigation of the morphology, composition and structure of molybdenum and molybdenum carbide films;

(3) Development of realistic models to simulate evaporation, chemical reaction and the deposition process.

Task 1. Study of Molybdenum Carbide Electrodeposition from Oxide Based Molten Salts

Characterization of deposition process

The electrochemical plating cell assembly (Figure 1) consists of a low-carbon steel cathode, a graphite or molybdenum anode, and a platinum flag as a quasi-reference electrode. Cylindrical cathodes of 3.1 or 6.3 mm dia and about 30 mm length were cut from a low-carbon steel rod (AISI 1018). They were initially etched with 10 % hydrochloric acid followed by rapid rinsing by water and acetone. Later, they were cleaned mechanically using successively finer grades of silicon carbide paper (240, 320, 400, 600), and then rinsed again by alcohol and water. Next, in most cases, they were polished with Alfa Micropolish Alumina Solution - 1.0 μm (Buehler), followed by a final ultrasonication in alcohol and acetone.

A molten salt bath consisting of an equimolar mixture of Na_2WO_4 and K_2WO_4 was used. The molybdenum and carbon species were introduced as alkali molybdate and carbonate, by direct mixing with the base tungstates as a powder. Initially all individual components were dried at 200-300 °C for 2-3 hours in order to remove as much moisture as possible from the commercially available laboratory chemicals. Following this procedure, the melt components were weighed and mixed to give the desired electrolyte composition.

The pre-dried powder mixture was heated slowly to about 600 °C at which temperature the electrolyte started to melt. One to two hours were necessary after melting to produce a clear melt. As a second step, in some cases additional electrochemical purification was carried out. To remove the remaining moisture completely, the melt was electrolyzed at about 1.5-2.0 V at 650 °C between two carbon electrodes until the current dropped to a low constant value typically less than 1 mA.

Next, the pre-electrolysis electrode assembly was replaced by plating electrodes and then these were slowly immersed in the molten electrolyte to avoid thermal shock. After reaching thermal equilibrium (usually in 1-1.5 hours), the temperature was raised slowly to the working temperature, 900 °C. Electrolysis was started within 1 hour after reaching this temperature. Following electrolysis the temperature was decreased again slowly, and at 600 °C the electrode assembly was removed. After complete cool-down, the electrodes were ultrasonically stripped

of adherent frozen melt.

Effect of Electrolyte Composition

The electrolyte bath composition was varied in order to study the influence of the kind and amount of alkali molybdate and carbonate on the resulting deposits and, on this basis to choose the optimal composition. Later, the process parameters of molybdenum and Mo_2C deposition from a fixed bath composition were studied in order to generate satisfactory coatings with reproducible surface topology and thickness.

Several different bath compositions have been utilized with approximately 8 - 10 mol% alkali molybdate and variable amounts of alkali carbonate. Table 1 lists the chemical compositions of the electrolyte baths used, whereas Table 2 shows the different plating conditions used. The working temperature was varied from 900 to 1100 °C. Below 850 °C no deposit was observed. Non-lithium electrolytes in all cases required higher working temperatures. Moreover, when adding borate the temperature had to be increased by 50 - 80 °C. It should be noted that larger grain sizes were found at higher temperatures.

The experiments performed without pre-electrolysis of the electrolyte gave, in most cases, irreproducible results. After pre-electrolysis, coatings of more-reproducible quality were obtained. Using non-lithium alkali molybdates and carbonates, coatings of even better quality were obtained. Adding 3-8 mol% $Na_2B_4O_7$ to the basic non-lithium bath composition was observed to cause significant morphology and quality improvements. These bath compositions produced a more uniform small-grain-size coating, which is a remarkable advantage. Moreover they do not require extensive purification because they are apparently not very sensitive to moisture in the atmosphere.

Significant information about the coating quality was obtained from examination of sample cross-sections. The best coating was obtained from non-lithium based pre-electrolyzed electrolyte using borate addition (Figure 2). Lithium-based electrolytes produced coatings with considerably lower quality and poor adhesion, especially in air atmosphere. However, for lithium-based electrolyte baths the borate addition and/or the use of inert atmosphere improve the quality and adhesion of the coatings obtained to a marked extent.

The sample cross-section shown in Figure 2 indicates approximately uniform thickness

over irregular substrate profiles and a virtually dense pore-free coating. The deposit seems to consist of two zones: a) a zone which constitutes the true molybdenum carbide coating; b) a Fe-Mo diffusion region most probably corresponding to molybdenum solid solution at the iron/molybdenum carbide interface. This assumption was confirmed by electron microprobe and X-ray diffraction measurements. Figure 3 represents typical concentration profiles for molybdenum and iron obtained by electron microprobe analysis for the sample shown in Figure 2. The X-ray diffraction data indicate the presence only of carbide in the outer layer of the coating in agreement with the interpretation of the microscopic cross-section picture.

Effect of Plating Current Modulation

Both constant current and reverse current patterns were applied during plating. The instrumentation consisted of an EG&G PAR Model 175 Universal Programmer, a Model 179 Potentiostat/Galvanostat provided with Model 179 Digital Coulometer plug-in option, a Hewlett-Packard ColorPro Plotter and a Nicolet 310 Explorer II Digital-Storage Oscilloscope.

Reverse-current plating was applied to achieve a certain grain structure and thickness. This procedure consisted of applying an initial cathodic current, I_c, followed by current reversal characterized by anodic current, I_a, with cathodic and anodic current flow times t_c and t_a respectively, where $t_c + t_a = t$ represent the full period of the reversing-current wave - see Figure 4. A very important characteristic of this plating mode is the ratio t_c/t_a ("duty cycle"). With proper t_c/t_a ratios, the reverse-current modulation produces smaller-grain-size coatings with better adhesion than the constant-current plating at the same working temperature. It also makes higher current densities possible and appears to be most effective in generating good-quality coatings.

In summary, it was found that good-quality well-adherent coatings of Mo_2C can be obtained under the following conditions:

electrolyte	Na_2WO_4 - K_2WO_4	80 - 90 wt%
	Na_2MoO_4	5 - 10 wt%
	Na_2CO_3	3 - 8 wt%
	$Na_2B_4O_7$	0.5 - 3 wt%
temperature		950 - 1000 °C
cathode substrate		low-carbon steel

anode material	carbon, molybdenum
cathodic current density	30 - 50 $mA.cm^{-2}$

Our preliminary investigations showed that in the absence of Na_2CO_3, and applying similar conditions, pure metallic molybdenum coatings with high quality can also be obtained (18).

Characterization of deposition mechanism

To get some insight into the processes taking place during the initial stages of molybdenum carbide electrodeposition, an analysis of the potentiostatic current transients in borate-free electrolyte was performed.

A typical current transient for molybdenum carbide deposition on iron substrate is shown in Figure 5. As can be seen, the transient is characterized by an initial current drop and subsequent current rise, which is connected with the formation of the new molybdenum carbide phase. The initial current decrease is due not only to the obviously double layer charge, but probably also to molybdenum incorporation into the iron substrate and formation of iron-molybdenum solid solution.

The analysis of the initial rising parts of the current transients shows that they follow a linear $i\text{-}t^{1/2}$ dependence as demonstrated in Figure 6. The deviation of the data from a straight line is probably caused by the current connected with the molybdenum solid solution formation. The linear $i\text{-}t^{1/2}$ dependence can be explained in terms of a model involving instantaneous nucleation and three-dimensional (3-D) diffusion-controlled growth. The corresponding current-time relation before the overlapping of the growing centers and/or their diffusion zones is given by the following equation (19,20):

$$i = NzF\pi(M/\rho)^{1/2}(2DC)^{3/2}t^{1/2} \qquad (1)$$

where D, C, and zF are respectively the diffusion coefficient, the electrolyte concentration, and the molar charge of the diffusing species, N is the number of nuclei formed at $t=0$, and M and ρ are the molecular weight and the density of the nearly deposited phase.

It could be assumed that in the case of molybdenum carbide electrodeposition on iron

substrates from tungstate based electrolytes (without borate addition) the nucleation proceeds on active sites at an extremely high rate and thus the nuclei are formed instantaneously at t=0. Further deposition is then controlled by the spherical diffusion of active species in the electrolyte. The influence of the substrate surface pre-treatment and of borate addition on the nucleation growth mechanism is interesting and may need to be studied further.

Conclusions

Dense, well-adherent molybdenum and molybdenum carbide coatings can be deposited from oxide-based melts. The coating morphology depends strongly on melt composition, temperature and moisture content. Initial pre-electrolysis significantly changes the composition and morphology of the coatings. Non-lithium electrolyte baths do not require extensive purification. Addition of $Na_2B_4O_7$ to the basic non-lithium bath causes marked morphology and quality improvements. Analysis of potentiostatic current transients can give important additional information about the nucleation and growth mechanism during the initial stages of molybdenum and molybdenum carbide electrodeposition.

Task 2. Preparation of Mo and Mo_2C by Plasma-Enhanced Chemical Vapor Deposition

Design of the Plasma Enhanced Chemical Vapor Deposition System

The PECVD inlet system, shown in Figure 7, has been constructed to allow safe conditions and procedures for the full duration of experiments. Like a every glow discharge system for thin film production, it is comprised of the following basic components:

(i) the reactor or deposition chamber;

(ii) an AC power generation source, usually at some fixed frequency; i.e., 13.56 MHz

(iii) an impedance matching network to transfer the power more efficiently from the generator to the gas load;

(iv) gas flow regulators (automatic or manual, such as a rotameter) and gas control section;

(v) pressure measurement plus other panel instrumentation.

In this project, a molybdenum deposit was prepared using molybdenum carbonyl as a precursor. The carbonyl is contained as a solid in the saturator reservoir, and its sublimation pressure is controlled by regulating the reservoir temperature. Thus, the desired dilution of carbonyl in carrier gas can be achieved relatively easily, because a temperature of only 25 - 100°C is required. The carrier gas (i.e., Ar, H_2, CH_4) can introduce molybdenum carbonyl vapor into the reaction chamber and maintain a stable plasma discharge. The inlet configuration is convenient to operate and easy to remove.

A glow discharge plasma is a relatively low-temperature, low-pressure gas in which a degree of ionization is sustained by high-energy electrons. Such a plasma was generated by using carrier gas and molybdenum carbonyl as precursor. The steady state plasma was generated by a RF power source applied after a stationary flow at approximately 0.2 to 2 torr pressure had been established. A heating system was installed in which the substrate is heated by a resistance heater, monitored by an embedded thermocouple. A maximum temperature could be obtained of about 350°C for the sample holder.

Evaporation of Molybdenum Carbonyl in the PECVD System

According to thermodynamics, vapor-solid equilibrium requires equality of the chemical

potentials of relevant components in the various phases and is characterized by a function which depends on the variables of overall pressure and temperature. The Clausius-Clapeyron equation permits calculation of the vapor pressure of molybdenum carbonyl as a function of temperature (see Table 3). It appears that concentrations of 5-50 mol% carbonyl at 0.1 - 2 torr total pressure can be obtained by controlling the temperature of the incoming carrier gas at between 10 and 50°C.

1. Chemical Equilibrium of Molybdenum Carbonyl in Evaporation

Since we intend to use thermodynamic calculations for the system Mo-C-O or Mo-C-O-(carrier gas) as a basis to understand the deposition process, it is useful to recall the theory on which this approach is based. The PECVD mechanism of molybdenum as well as molybdenum carbide is probably quite complicated, however as few as three reaction steps involving stable reactants and products can be selected and will suffice for thermodynamic analysis:

$$Mo(CO)_6(g) = Mo(s) + 6CO(g) \quad (R1)$$

$$2CO(g) = C(s) + CO_2 \quad (R2)$$

$$2Mo(s) + C(s) = Mo_2C \quad (R3)$$

Under various reaction conditions in the chamber, only three final solid products are possible: molybdenum, molybdenum carbide and carbon. Assuming that only $Mo(CO)_6$ decomposition (R1) takes place, the mole fractions and the equilibrium constant in the gas phase are as follows:

$$K = \frac{P^5(6X)^6}{(1-X)(1+5X)^5} \quad (2)$$

$$Y_{Mo(CO)_6} = \frac{1-X}{1+5X} \quad (3)$$

Here X is the extent of the decomposition of $Mo(CO)_6$. Equation 2 indicates that the extent of decomposition is very sensitive to the total pressure. The extent of decomposition can be obtained by a Newton iteration program. Typical results are shown in Figure 8. The extent of $Mo(CO)_6$ decomposition also increases with increasing temperature (see Figure 8 and Table 4).

2. Phase Equilibrium of Molybdenum Carbonyl

As we mentioned previously, the saturator temperature generally corresponds to a certain sublimation pressure of $Mo(CO)_6$. The ratio of the saturation pressure of $Mo(CO)_6$, P^{sat}, and the total pressure in the reaction chamber, P, appears to have an important effect on the vapor deposition process. This can be analyzed from a thermodynamic viewpoint. For example, a metallic sheet is to be coated with a thin layer of solid A. To do so, it is proposed to vaporize the solid and to allow the vapor to condense on the sheet in an isolated chamber. A simple model CVD system is shown in Figure 9. If there is local equilibrium for precursor A, at temperature T and pressure P, then:

$$f_A^s = f_A^v \tag{4}$$

where superscript v stands for the gas phase and s stands for the solid phase.

Because the solid phase is pure, its fugacity is given by

$$f_A^s = P_A^s \phi_A^s \exp\left(\int_{P_A^{sat}}^{P} \frac{v_A^s dP}{RT}\right) \tag{5}$$

P_A^s is the saturation vapor pressure of pure solid, Φ_A^s is the fugacity coefficient at saturation pressure P_A^v and v_A^s is the solid molar volume, at all temperature T.

For the vapor phase fugacity,

$$f_A^v = \phi_A y_A P \tag{6}$$

We can obtain the mole fraction in the gas phase,

$$y_A = \frac{P^s}{P} E \tag{7}$$

where

$$E=\frac{\phi_A^s \exp\left(\int_{P_A^s}^{P} \frac{v_A^s dP}{RT}\right)}{\phi_A} \tag{8}$$

The quantity E, is nearly always greater than unity, and is therefore called the enhancement factor; that is, E is the correction factor which must be applied to the simple (ideal-gas) expression that is valid only at low pressure. The enhancement factor is a measure of the extent to which pressure enhances the mole fraction in the gas; as $P \rightarrow P_A^s$, $E \rightarrow 1$. The saturation pressure P_A^s of the solid is small and thus Φ_A^s is nearly equal to unity.

Here y_A, the mole fraction of precursor in the gas phase, is proportional to P^s/P, so the larger the ratio of saturation pressure to total pressure, the larger the mole fraction of $Mo(CO)_6$ in the gas phase. There is good agreement between these predictions and the experimental data. This result means that favorable conditions are created for Mo and Mo_2C deposition by increasing P^{sat}/P.

3. Evaporation Rate of Molybdenum Carbonyl

The theoretical maximum evaporation rate can be obtained only if as many evaporant molecules leave the surface as would be the case if the equilibrium pressure p^* on the same surface is exerted, while none of them return. This evaporation rate is equal to the impingement rate which, according to kinetic theory, is related to temperature and pressure as follows:

$$\Gamma = m\frac{dN_e}{A_e dt} = \left(\frac{m}{2\pi kT}\right)^{1/2} p^* \tag{9}$$

or

$$\Gamma = 5.834 x 10^{-2} \left(\frac{m}{T}\right)^{1/2} p^* \tag{10}$$

for mass evaporation rate in ($g/sec.cm^2$) and pressure in torr.

Based on these considerations, the number of molecules dN_e evaporating from a surface area A_e during the time dt is equal to the impingement rate at the equilibrium (or saturation) pressure p^*, minus a return flux corresponding to the partial pressure p of the evaporant in the bulk gas phase:

$$\frac{dN_e}{A_e dt} = \alpha_v (2\pi mkT)^{-1/2}(p^* - p) \qquad (11)$$

This is commonly referred to as the Hertz-Knudsen equation. α_v is evaporation coefficient. For $\alpha_v = 1$ and $p = 0$, the maximum evaporation rate results.

Assuming a uniform rate across the entire evaporation area and no variation with time, mass evaporation can be determined from experimental data and inserted into equation (10) to obtain vapor pressure. We also can make a theoretical calculation of the mass evaporation rate from a function representing saturation pressure, such as the Clausius-Clapeyron equation.

A typical experimental result for $Mo(CO)_6$ evaporation (without applying RF power) is shown in Figure 10. If we assume decomposition of $Mo(CO)_6$ (equation R1) to occur in the vacuum chamber, one can deduce the partial pressure of $Mo(CO)_6$ in the bulk gas by applying the Hertz-Knudsen equation. By this means, one can calculated that the partial pressure of molybdenum carbonyl is about 0.105 torr at 22°C. Further analysis of $Mo(CO)_6$ evaporation is in progress.

Preparation of Thin Film by PECVD

An effort has been undertaken to deposit Mo and Mo_2C thin film on a substrate of 1-in by 1.5-in area. The following experimental parameters were varied: pressure(P), temperature (T), RF power, time, and gas flow. To limit the number of experiments, a statistical design based on the orthogonal table for 5 variables at 2 levels was used (see Table 6). The actual parameters are shown in Table 5. Two basically different conditions emerge from Table 3: vacuum evaporation, i.e., zero flow rate (level 1); and forced convection (level 2). To estimate the approximate deposition rate of Mo or Mo_2C and the evaporation rate of molybdenum

carbonyl, the substrate and the molybdenum carbonyl precursor were weighed (precision 10^{-4} gram) before and after the discharge process.

Initial conclusions have been drawn from the weight gain of the substrate about the optimal conditions for maximum deposition. The results are shown in Figure 11. The analysis shows clearly that the factor which affects the deposition rate most is the flow rate of argon gas. This is understandable since the deposition rate may be increased strongly if introducing argon carrier gas into the reaction chamber can be avoided, because the argon gas dilutes the concentration of $Mo(CO)_6$ and decreases the deposition rate. The above results indicate that it is possible to depend on direct evaporation of $Mo(CO)_6$, i.e., $Mo(CO)_6$ is used as a discharge medium instead of using argon gas.

The second factor is the pressure in the reaction chamber. As the pressure is lowered, the deposition rate increases, because the lower total pressure makes the rate of increase of concentration of molybdenum carbonyl in the chamber higher. A third factor is the temperature and power density in the chamber. If the temperature and power density increase, the concentration of radicals and gaseous ions also increases. This should increase the deposition rate by increasing the evaporation rate. The deposition time is an independent factor. It is expected to play a minor role as long as deposition of Mo_2C takes place at a much smaller rate than evaporation of $Mo(CO)_6$.

Conclusions

Several important process considerations have been identified. Some can only be stated as empirical rules. Application of these ideas depends upon the material and reactor design being considered, but they are stated below, by way of conclusions, in a general form.

(i) The distinguishing feature of plasma enhanced CVD is electron impact dissociation of reactants, where the reaction surface is in contact with the plasma.

(ii) The plasma deposition technique described here is a chemical deposition from reactive species in the vapor above the film. The plasma energy can assist thermal energy supplied by the substrate to overcome the kinetic limitation of otherwise (thermodynamically) favored deposition reactions. Film composition and deposition rate are sensitive to the reactant gas and free radical concentration in the region of deposition.

(iii) Plasma enhanced CVD has many process variables: power, pressure, substrate temperature, gas flow rate and flow ratios. While the number of variables makes the process complicated, it allows the process to be adjusted for control of film properties and for uniform deposition. The optimization of parameters in the present case points to low flow rate of carrier gas in the reaction chamber, low pressure, high power density, and moderately high temperature as favorable conditions. Amorphous films, from a few tens to a few hundreds of nm thick, have been obtained on glass and steel as substrates.

REFERENCES

1. J. L. Andrieux and G. Weiss, Bull. Soc. Chim. France, 598 (1948).
2. H. T. Heinen, C. L. Barber and D. H. Baker, US Bur. Mines, Rep. Invest., 6590 (1965).
3. A. D. Graves and D. Inman, Electropl. Metal Finish., 19 (1966) 314.
4. S. Senderoff and G. W. Mellors, J. Electrochem. Soc., 114 (1967) 586.
5. F. X. McCawley, C. Wyche and D. Schlain, J. Electrochem. Soc., 116 (1969) 1028.
6. A. K. Suri, T. K. Mukherjee and C. K. Gupta, J. Electrochem. Soc., 120 (1973) 622.
7. A. N. Baraboshkin et al., Elektrokhimia, 13 (1977) 1807.
8. K. H. Stern, US. Patent 4 430 170 (1984).
9. K. Koyama, Y. Hashimoto and K. Terawaki, J. Less-Comm. Metals, 134 (1987) 141.
10. D. C. Topor and J. R. Selman, J. Electrochem. Soc., 135 (1988) 384.
11. G. J. Kipouros and D. R. Sadoway, J. Appl. Electrochem., 18 (1988) 823.
12. V.I. Shapoval, Kh.B. Khushkov and I.A. Novoselova, Ukr. Khim. Zh., 48 (1982) 738.
13. V.I. Shapoval, Kh.B. Khushkov, V.V. Malyshev, P.V. Nazarenko and N.P. Baidan, Zashch.Met., 22 (1986) 564.
14. V. I. Shapoval, A. N. Baraboshkin and Kh. B. Kushkov, Elektrokhimia, 23 (1987) 885.
15. V.I. Shapoval, Kh.B. Khushkov, V.V. Malishev, V.T. Vesna and V.P. Maslov, Poroshk. Metall. (Kiev), 7 (1987) 43.
16. V.A. Polishchuk, Kh.B. Khushkov and V.I. Shapoval, Electrokhimia, 26 (1990) 305.
17. B. Aladjov, P. Yankulov, P. Angelov, K. Khushkov and G. Staikov, Proc. DOE/EPRI Beta Battery Workshop VIII, Chester, UK, June 11-13 (1990) 29-1.
18. B. Aladjov, D. Topor and J.R. Selman, Electrochem. Soc. Spring Meeting, St.Louis, Missouri, May 17-22, 1992, Extended Abstracts, vol. 92-1, p. 792.
19. J.A. Harrison and H.R. Thirsk, in Electroanal. Chem. (Ed. A. Bard), Marcel Dekker, New York, vol. 5 (1971) p.67.
20. G.J Hills, D.J. Schiffrin and J. Thompson, Electrochim. Acta, 19 (1974) 657.
21. J.J Lander and L.H Germer, Trans AIME 175 (1948) 648

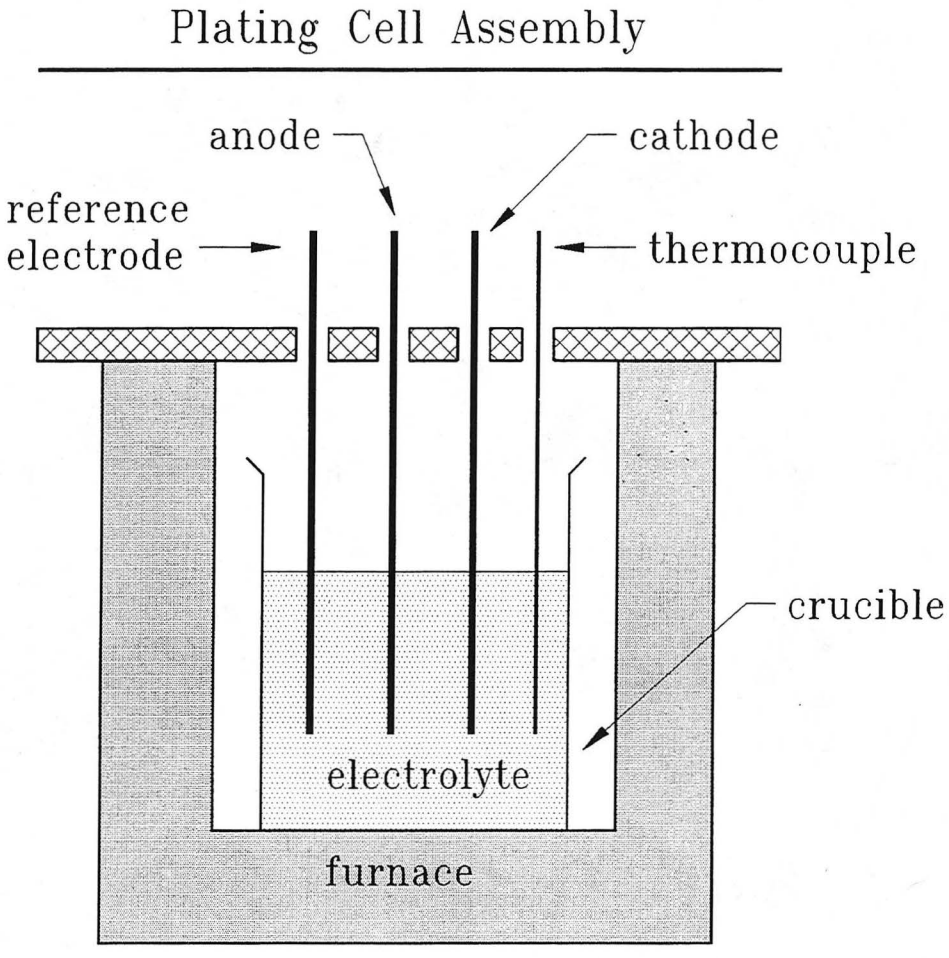

Figure 1. Electrochemical Plating Cell Assembly

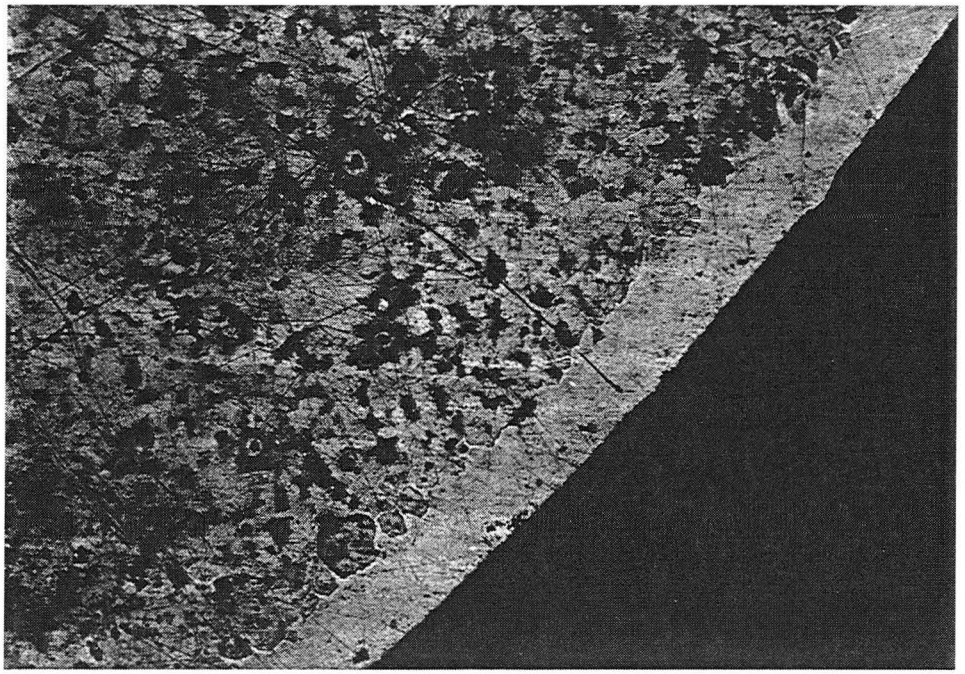

Figure 2. Cross-section of a sample prepared under condition Q, according to Table 2, working temperature at 1000°C

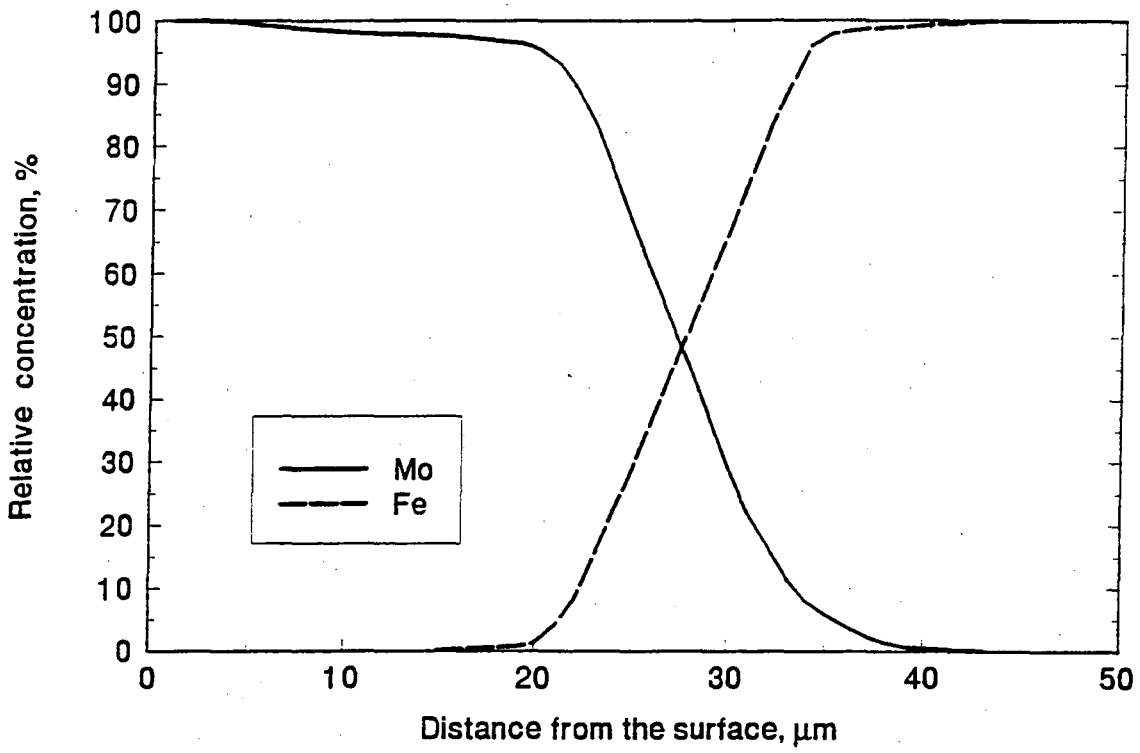

Figure 3. Concentration profiles from molybdenum and iron in a molybdenum carbide coated low-carbon steel sample shown in Figure 2.

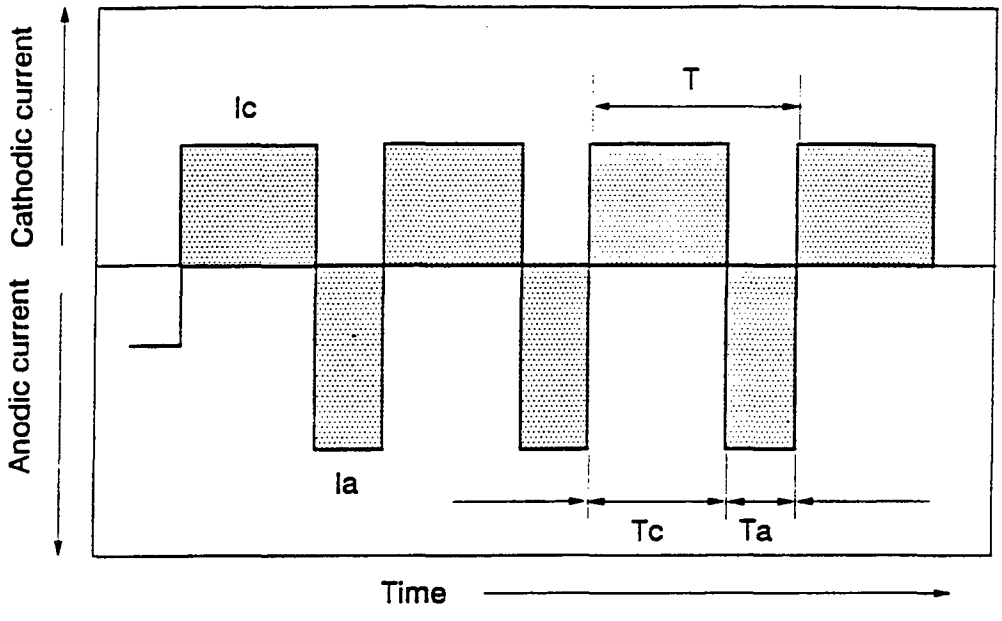

Figure 4. Current modulation applied during the reverse electrolysis

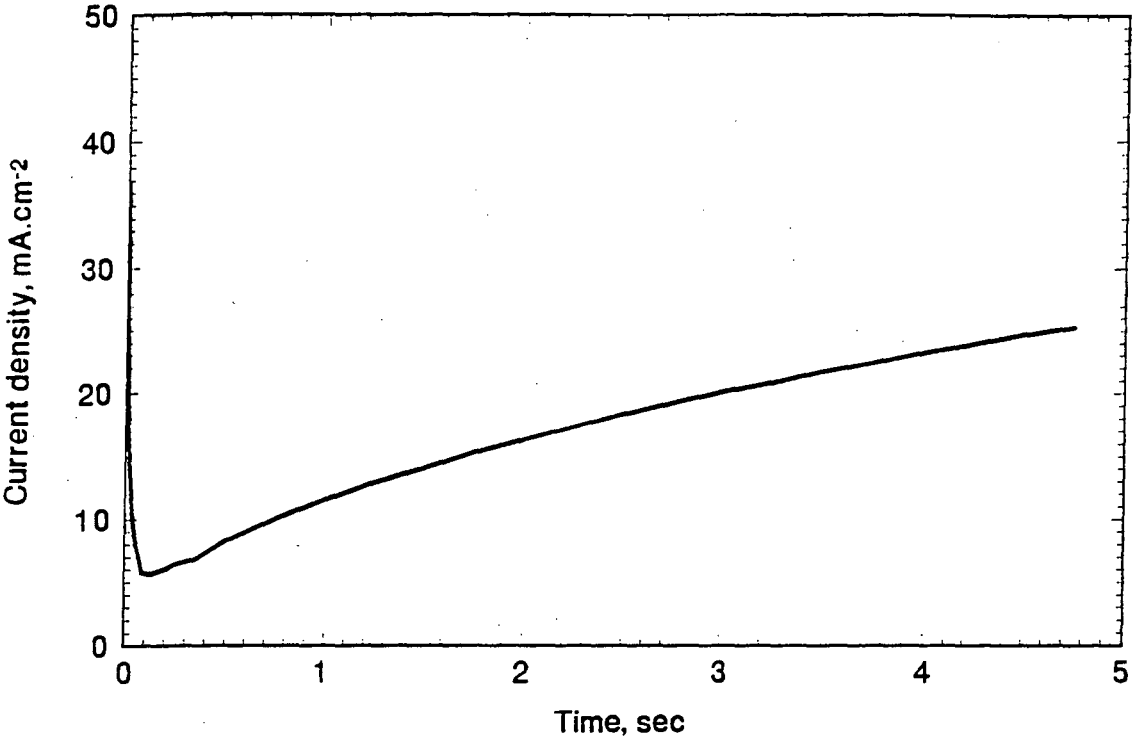

Figure 5. Typical current transient for molybdenum carbide deposition obtained at 40 mV and 1000°C under condition H, according to Table 2.

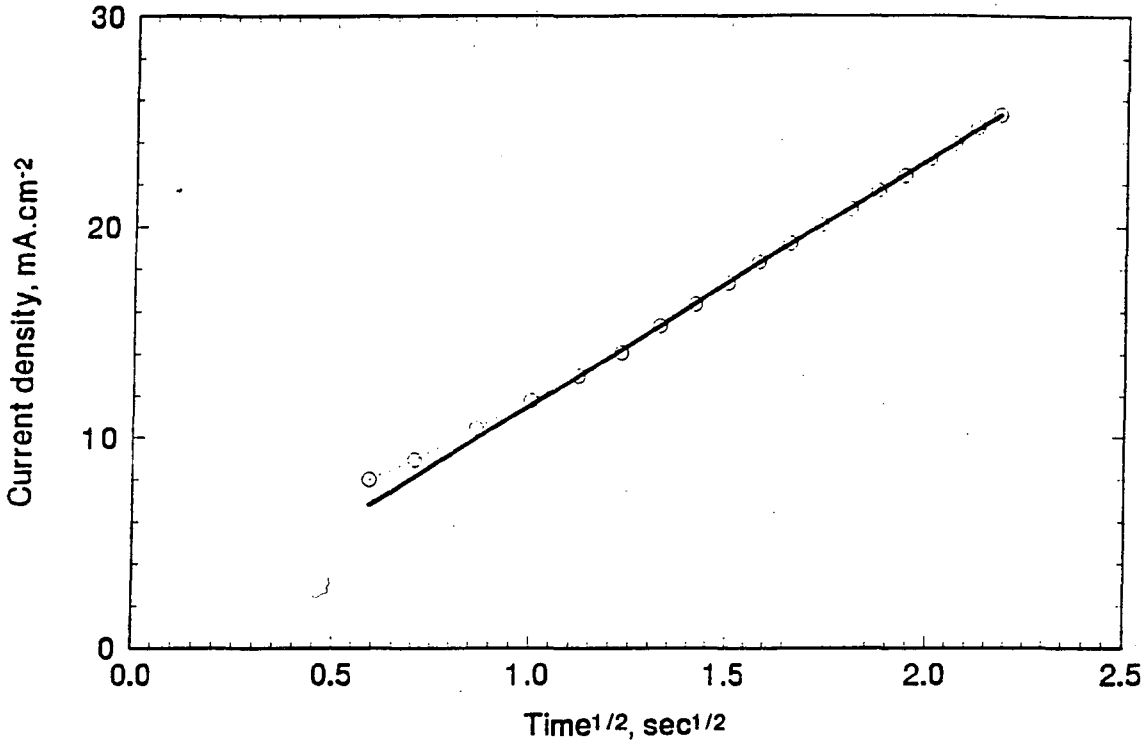

Figure 6. Current density vs. square root of time plot of the rinsing part of the transient shown in Figure 5.

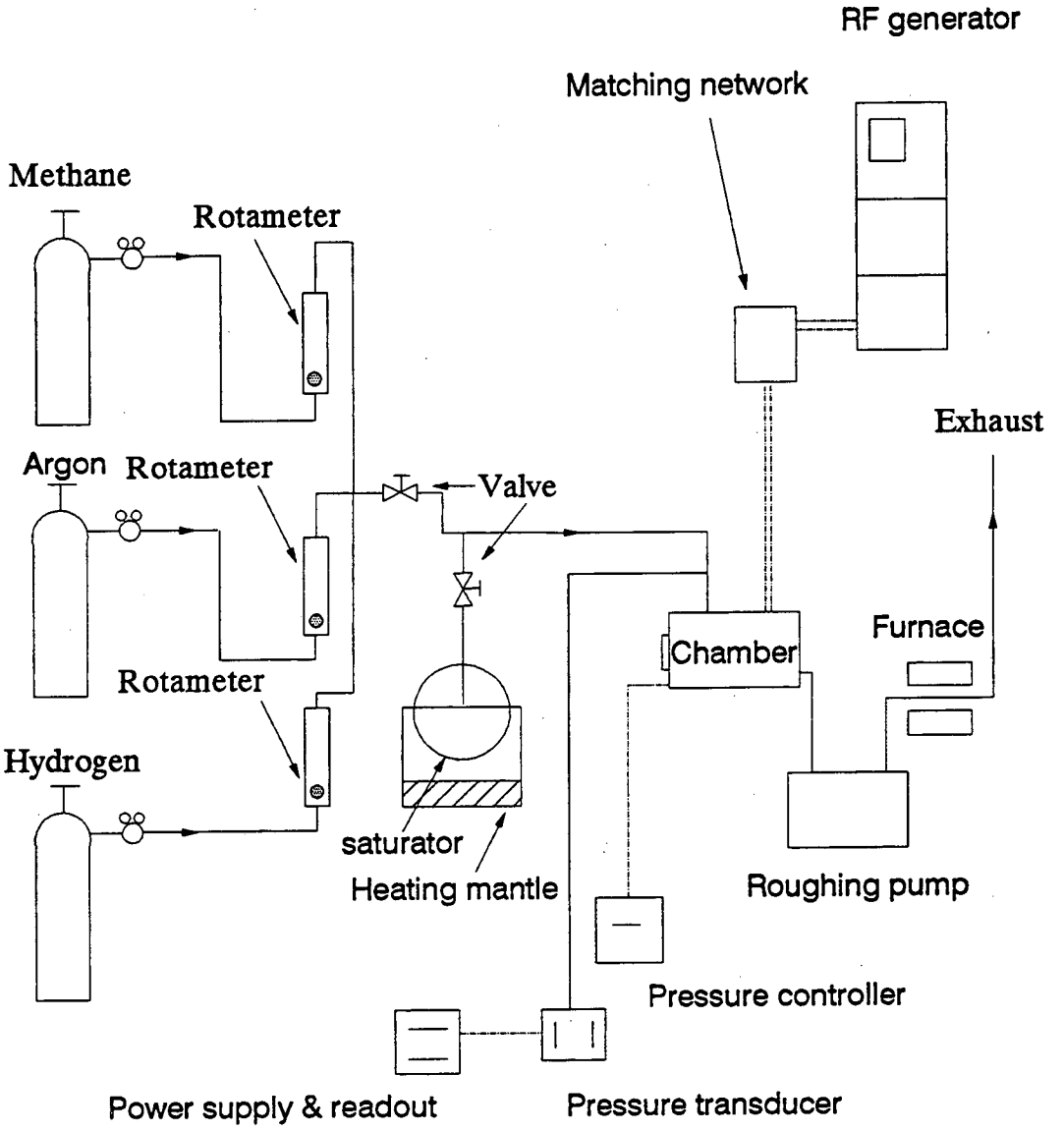

Figure 7. Schematic of inlet configuration

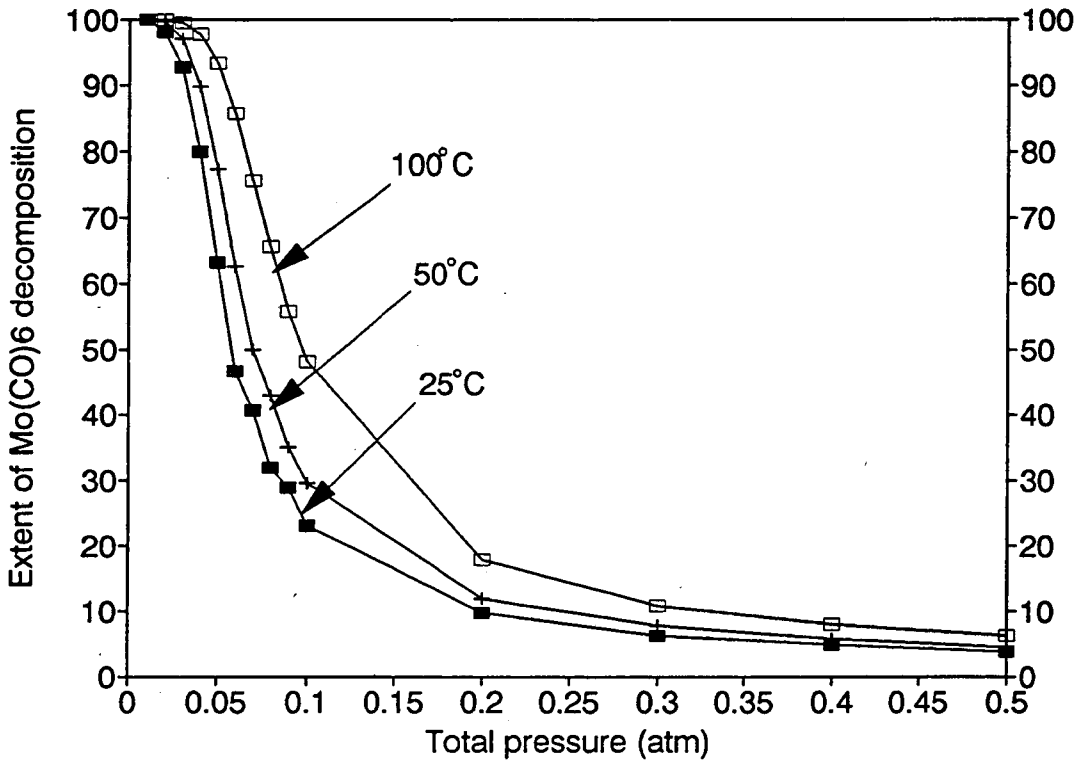

Figure 8. The extent of $Mo(CO)_6$ decomposition

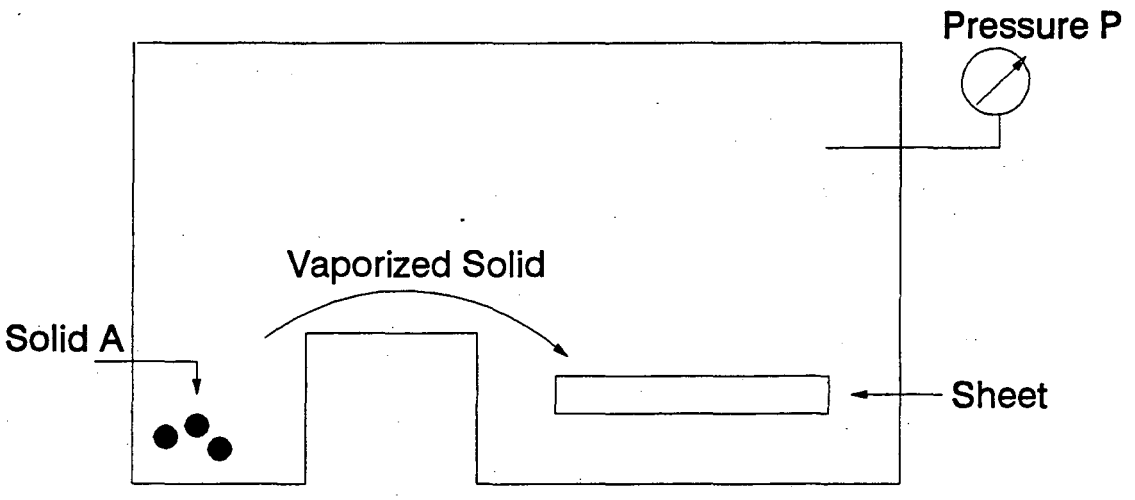

Figure 9. A simply CVD system assuming local equilibrium of the precursor vapor pressure

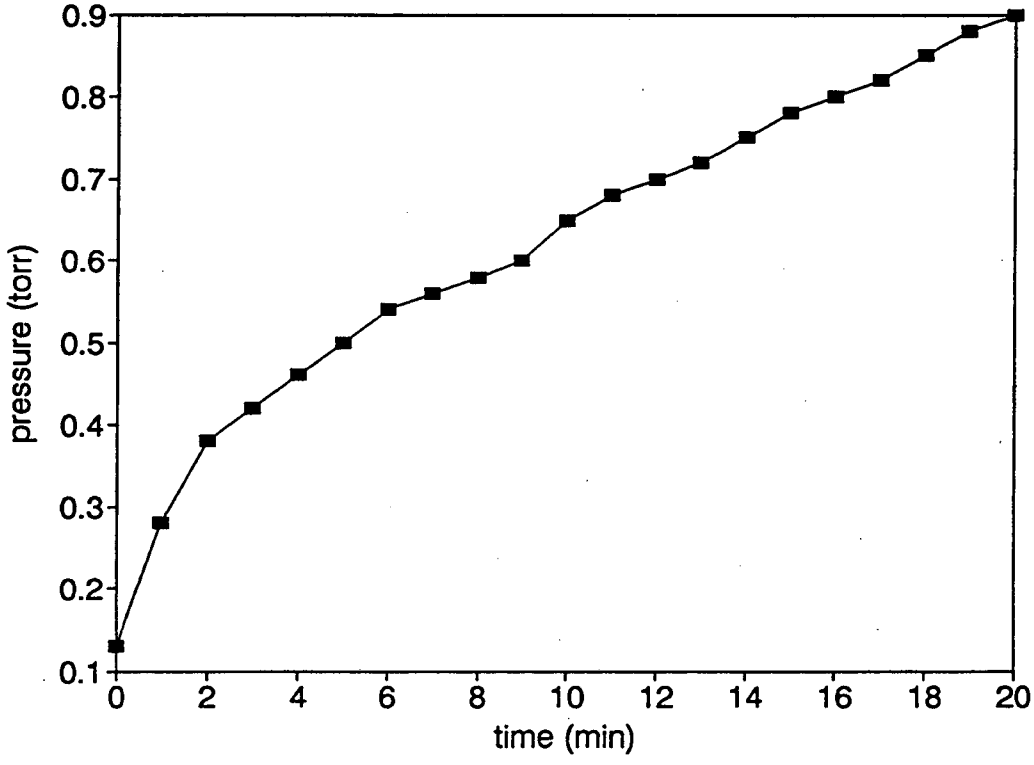

Figure 10. $Mo(CO)_6$ evaporation in PECVD system

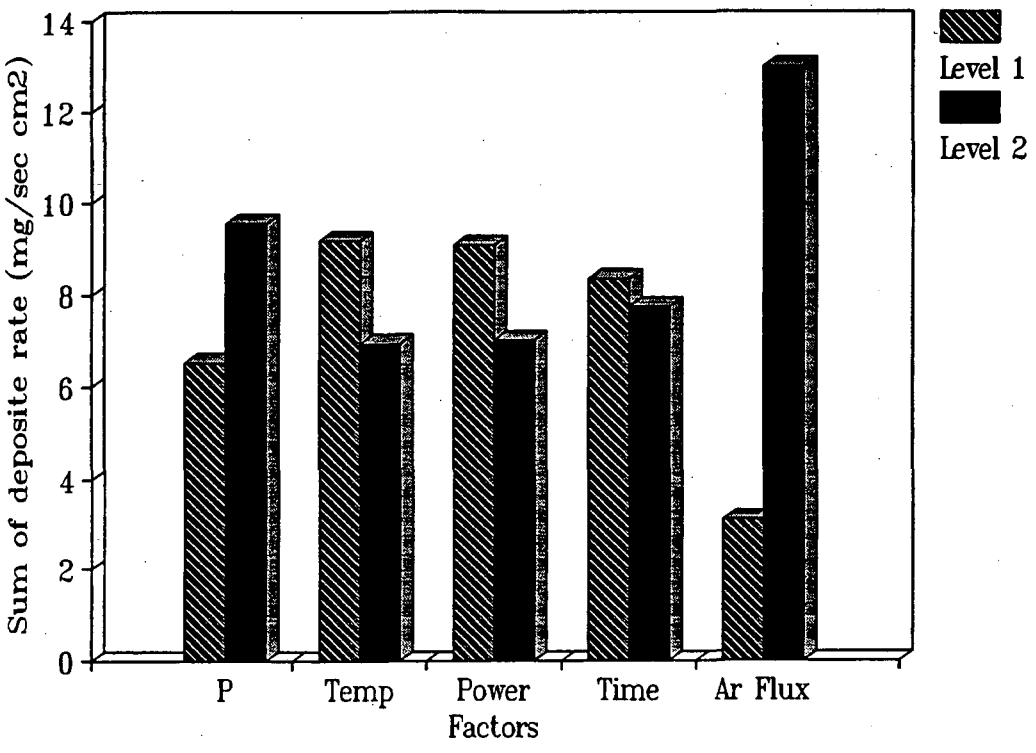

Figure 11. Effect of operating parameters on deposition rate

Table 1. Chemical composition of the electrolyte bath used in the plating experiments. Major bath components are indicated for each experiment.

	1	2	3	4	5	6	7	8	9	10	11	12	13	14
Na2WO4	●	●	●	●	●	●	●	●	●	●	●	●	●	●
K2WO4	●	●	●	●	●	●	●	●	●	●	●	●	●	●
Li2MoO4	●	●	●											●
Na2MoO4				●	●	●					●			
K2MoO4							●	●	●			●		
MoO3										●			●	
Li2CO3	●			●			●			●				●
Na2CO3		●			●			●			●		●	
K2CO3			●			●			●			●		
Na2B4O7											●	●	●	●

Table 2. Different plating conditions in MSECD from oxide baths

		Without Pre-electrolysis		Pre-electrolysis	
		Glove box	Outside	Glove box	Outside
Without additions	Lithium baths	A	B	C	D
	Non-lithium baths	E	F	G	H
Borate additions	Lithium baths	I	K	L	M
	Non-lithium baths	N	O	P	Q

Table 3. Molybdenum carbonyl pressure data

K	°C	log P, mmHg	P, mmHg
293	20	-1.065	0.086
298	25	-0.856	0.139
303	30	-0.653	0.222
308	35	-0.456	0.348
313	40	-0.268	0.539
318	45	-0.084	0.824
323	50	0.093	1.239
333	60	0.433	2.710
343	70	0.753	5.662
353	80	1.055	11.35
363	90	1.34	21.878
373	100	1.61	40.738

$Mo(CO)_6$ solid, m.p. = 152°C with decomposition.

Low temperature values calculated using the equation [21]:

$$\log P\ (mmHg) = 11.406 - 3654/T(K)$$

Table 4. Calculated extent of $Mo(CO)_6$ decomposition

	25°C	50°C	100°C
Pt (atm)	Extent(%)	Extent(%)	Extent(%)
0.5	3.8	4.52	6.26
0.4	4.74	5.64	7.91
0.3	6.23	7.76	10.87
0.2	9.73	11.91	17.81
0.1	23.08	29.49	48.01
0.09	28.93	35.03	55.77
0.08	31.82	42.82	65.48
0.07	40.57	49.85	75.59
0.06	46.55	62.46	85.64
0.05	63.11	77.34	93.20
0.04	79.92	89.81	97.60
0.03	92.7	96.99	99.40
0.02	98.0	99.61	99.92
0.01	99.97	99.99	99.99

Table 5. Design Parameters for a 5-variable 2-level Test Design

Factors	P	T	Power	t	Flux
Level 1	2	50	40	40	100
Level 2	0.5	25	20	20	0
Unit	(torr)	(°C)	(Watt)	(min)	(sccm)
1	2	50	40	20	0
2	0.5	50	20	20	100
3	2	25	20	20	0
4	0.5	25	40	20	100
5	2	50	20	40	100
6	0.5	50	40	40	0
7	2	25	40	40	100
8	0.5	25	20	40	0

Table 6. Standard Orthogonal Test Table

Col No.	1	2	3	4	5	6	7
Ex No.							
1	1	1	1	2	2	1	2
2	2	1	2	2	1	1	1
3	1	2	2	2	2	2	1
4	2	2	1	2	1	2	2
5	1	1	2	1	1	2	2
6	2	1	1	1	2	2	1
7	1	2	1	1	1	1	1
8	2	2	2	1	2	1	2

LAWRENCE BERKELEY LABORATORY
UNIVERSITY OF CALIFORNIA
TECHNICAL INFORMATION DEPARTMENT
BERKELEY, CALIFORNIA 94720